

# Critical behavior near the Mott transition in the half-filled asymmetric Hubbard model



Anh-Tuan Hoang<sup>a,\*</sup>, Duc-Anh Le<sup>b</sup>

<sup>a</sup> Institute of Physics, Vietnam Academy of Science and Technology, Hanoi, Vietnam

<sup>b</sup> Faculty of Physics, Hanoi National University of Education, Xuan Thuy 136, Cau Giay, Hanoi 10000, Vietnam

## ARTICLE INFO

### Article history:

Received 16 June 2015

Received in revised form

16 December 2015

Accepted 16 January 2016

Available online 20 January 2016

### Keywords:

Mott-insulator

Asymmetric Hubbard model

Dynamical mean field theory

## ABSTRACT

We study the half-filled asymmetric Hubbard model within the two-site dynamical mean field theory. At zero temperature, explicit expressions of the critical interaction  $U_c$  for the Mott transition and the local self-energy are analytically derived. Critical behavior of the quasiparticle weights and the double occupancy are obtained analytically as functions of the on-site interaction  $U$  and the hopping asymmetry  $r$ . Our results are in good agreement with the ones obtained by much more sophisticated theory.

© 2016 Elsevier B.V. All rights reserved.

## 1. Introduction

The Mott metal–insulator transition (MIT) is a fundamental problem in the theory of strongly correlated electron systems. Theoretical works on the MIT have mainly focused on the Hubbard model (HM) and the Falikov–Kimball model (FKM) [1–3]. The natural connection between these two models is the asymmetric Hubbard model (AHM), where each spin species has a different hopping amplitude and a different value of the chemical potential. The Hamiltonian of the model is

$$H = - \sum_{\langle ij \rangle, \sigma} t_{\sigma} (c_{i\sigma}^{\dagger} c_{j\sigma} + \text{H. c.}) - \sum_{i\sigma} \mu_{\sigma} n_{i\sigma} + U \sum_i n_{i\uparrow} n_{i\downarrow}, \quad (1)$$

where  $c_{i\sigma} (c_{i\sigma}^{\dagger})$  annihilates (creates) an electron with spin  $\sigma$  at site  $i$ ,  $n_{i\sigma} = c_{i\sigma}^{\dagger} c_{i\sigma}$ .  $\mu_{\sigma}$ ,  $t_{\sigma}$  and  $U$  denote the chemical potential, the nearest neighbor hopping parameter and the on-site Coulomb repulsion, respectively; the asymmetry parameter is defined as  $r = t_i/t_j$ . The limits  $r=0$  and  $r=1$  correspond to the FKM and the HM, respectively. It should be noted that the AHM is also used for a description of two-component fermionic mixtures loaded in an optical lattice [4–6]. In this case the index  $\sigma$  refers to the light and the heavy fermionic species,  $t_i \neq t_j$  implies fermionic mixtures having mass imbalance.

The dynamical mean field theory (DMFT), which becomes exact in the limit of infinite spatial dimensions, has been developed for the physics of strongly correlated electron systems. In the DMFT,

the original lattice model is mapped onto an effective single impurity Anderson model (SIAM) embedded in an uncorrelated bath of conduction electrons. The problem is then to find an appropriate solver for the effective impurity model and for this problem various methods employed for an essentially exact solution already exist [7–9]. Recently, the DMFT with different standard numerical impurity solvers, the numerical renormalization group (NRG), the Hirsch–Fye quantum Monte Carlo algorithm (HF-QMC) and the exact diagonalization method (ED), has been used to study the phase diagram of the AHM [10–12]. Various physical properties of this system, in particular, the paramagnetic phase diagram of the model as a function of temperature, the interaction and the hopping asymmetry were obtained. It can be seen that these numerical methods work well for the AHM, but they cost a lot of CPU time and resources, even if the system is half-filled and the chemical potential is known analytically. In addition, it is very difficult to obtain the critical behavior of the MIT numerically as the quasiparticle peak become very sharp in the vicinity of the MIT. It is thus important to find an approach that does not require much computational effort and gives a correct qualitative picture of the MIT in the asymmetric Hubbard model, including its critical behavior.

The two-site DMFT was proposed by Potthoff [13], who showed that a minimum realization of the DMFT is achieved by mapping a correlated lattice model onto an impurity model that consists of two sites, one for the impurity and one for the bath of conduction electrons. This method provides a simple and attractive technique to obtain fairly good results for the Mott transition and the Fermi liquid phase in the single band HM. The two-site DMFT was also successfully applied for studying the critical behavior of the MIT in

\* Corresponding author.

E-mail address: [hatuan@iop.vast.ac.vn](mailto:hatuan@iop.vast.ac.vn) (A.-T. Hoang).

the single- and the two-band Hubbard model [14–16]. Here we study the half-filled asymmetric Hubbard model within the two-site DMFT. The aim of the present paper is two-fold. First, we show that the two-site DMFT is able to catch the physics of the Mott transition and the Fermi liquid phase in the half-filled AHM. The second aim of this paper is to study the critical behavior of the quasi-particle weights and the double occupancy near the Mott transition. As far as we know, in the present literature there are two well-known simple approximations, the coherent potential approximation (CPA) [3,17] and the two-site DMFT [13], are well suited for studying the MIT in the symmetric HM and FKM, i.e. in the limiting cases of the AHM. However, the CPA has failed to be a successful theory for the asymmetric Hubbard model as pointed out in Ref. [18]. Therefore, the consideration of the reliability of the two-site DMFT for the AHM is necessary and far from trivial. The structure of the paper is as follows. In Section 2 we present the theoretical formulation. In Section 3 we calculate the critical interaction, the quasi-particle weight, the double occupancy and compare with the full DMFT. The critical behavior near the Mott MIT is obtained and discussed in Section 4. Finally, the conclusions are presented in Section 5.

## 2. Theoretical formulation

In the DMFT, the Hamiltonian model (1) is mapped onto an effective single impurity Anderson model

$$H_{\text{imp}} = \sum_{k\sigma} \varepsilon_{k\sigma} c_{k\sigma}^\dagger c_{k\sigma} + \sum_{k\sigma} (V_{k\sigma} c_{k\sigma}^\dagger d_\sigma + \text{H. c.}) - \sum_{\sigma} \mu_{\sigma} n_{d\sigma} + U n_{d\uparrow} n_{d\downarrow}, \quad (2)$$

where  $d_\sigma$  and  $d_\sigma^\dagger$  are the impurity operators with spin  $\sigma$  and  $\varepsilon_{k\sigma}$  is the energy of conduction electrons hybridized with the impurity by  $V_{k\sigma}$ . The effective parameters  $\varepsilon_{k\sigma}$  and  $V_{k\sigma}$  enter the hybridization function as

$$\Delta_\sigma(\omega) = \sum_k \frac{V_{k\sigma}^2}{\omega - \varepsilon_{k\sigma}}. \quad (3)$$

The on-site Green function for the lattice model (1) is given by

$$G_\sigma(\omega) = G_{ii\sigma}(\omega) = \int_{-\infty}^{+\infty} \frac{\rho_\sigma^0(z) dz}{\omega - (z - \mu_\sigma) - \Sigma_\sigma(\omega)}, \quad (4)$$

where  $\Sigma_\sigma(\omega)$  is the local self-energy. For the Bethe lattice with an infinite coordination number, we use the semicircular bare density of states

$$\rho_\sigma^0(z) = \frac{1}{2\pi t_\sigma^2} \sqrt{4t_\sigma^2 - z^2} \quad (5)$$

for which the self-consistent condition has the simple form

$$\Delta_\sigma(\omega) = t_\sigma^2 G_\sigma(\omega). \quad (6)$$

In the two-site DMFT, the hybridization function (3) can be represented by a single pole at  $\omega = 0$

$$\Delta_\sigma(\omega) = \frac{V_\sigma^2}{\omega}. \quad (7)$$

The AHM with Eq. (7) corresponds to the following two-site Anderson model:

$$H_{2\text{-site}} = \sum_{\sigma} \varepsilon_{c\sigma} c_\sigma^\dagger c_\sigma + \sum_{\sigma} V_\sigma (c_\sigma^\dagger d_\sigma + d_\sigma^\dagger c_\sigma) + \sum_{\sigma} \varepsilon_{d\sigma} d_\sigma^\dagger d_\sigma + U n_{d\uparrow} n_{d\downarrow}. \quad (8)$$

Here for the symmetric case of half-filling  $n = 1$ ,  $\mu_\uparrow = \mu_\downarrow = U/2$ , we

choose  $\varepsilon_{c\sigma} - \varepsilon_{d\sigma} = U/2$  to ensure the first self-consistency equation  $n = n_{\text{imp}}$ . The hybridization  $V_\sigma$  has to be determined from the second self-consistency equation:

$$V_\sigma^2 = Z_\sigma t_\sigma^2, \quad (9)$$

where  $Z_\sigma$  is the residue of the Green function  $G_\sigma(\omega)$  near  $\omega = 0$  and has the meaning of the quasi-particle weight.

At zero temperature, the two-site model (8) is solved analytically to obtain the impurity Green function with the form (see Appendix A)

$$G_\sigma(\omega) = \sum_{i=1,2} \left( \frac{z_{i\sigma}}{\omega - \varepsilon_{i\sigma}} + \frac{z_{i\sigma}}{\omega + \varepsilon_{i\sigma}} \right), \quad (10)$$

where the residues  $z_{i\sigma}$  and energy poles  $\varepsilon_{i\sigma}$  are (up to second order in  $V_\sigma/U$ ,  $\sigma = \uparrow, \downarrow$ )

$$z_{1\sigma} = \frac{1}{2} - \frac{2(V_\sigma + 2V_\sigma)^2}{U^2}, \quad (11)$$

$$z_{2\sigma} = \frac{2(V_\sigma + 2V_\sigma)^2}{U^2}, \quad (12)$$

$$\varepsilon_{1\sigma} = \frac{U}{2} + \frac{2[V_\sigma^2 + (V_\sigma + V_\sigma)^2]}{U}, \quad (13)$$

$$\varepsilon_{2\sigma} = \frac{2V_\sigma(V_\sigma + 2V_\sigma)}{U}. \quad (14)$$

When  $V_\uparrow, V_\downarrow \rightarrow 0$ , low energy poles merge together at  $\pm\varepsilon_{2\sigma} \approx 0$  with the total residue

$$Z_\sigma = \frac{4(V_\sigma + 2V_\sigma)^2}{U^2}. \quad (15)$$

Combining (9) and (15) yields two linear equations for  $V_\uparrow, V_\downarrow$

$$V_\uparrow = \frac{2t_\uparrow}{U}(V_\uparrow + 2V_\downarrow), \quad (16)$$

$$V_\downarrow = \frac{2t_\downarrow}{U}(2V_\uparrow + V_\downarrow). \quad (17)$$

Their determinant must vanish when  $U \rightarrow U_c^+$ , signaling a metallic phase. Therefore, the critical value for the MIT is given by

$$U_c = t_\uparrow + t_\downarrow + \sqrt{t_\uparrow^2 + t_\downarrow^2 + 14t_\uparrow t_\downarrow}. \quad (18)$$

The above expression of  $U_c$  is equivalent to Eq. (11) in Ref. [10], keeping in mind that in [10]  $D = (D_h + D_l)/2$ . Setting  $t_\uparrow = t_\downarrow = t$  in (18), this yields  $U_c = 6t$  and we reproduce the result of the HM obtained from the linearized DMFT by Bulla and Potthoff [14]. We also note that our result clearly improves on those of the generalized Hubbard-III approximation in Ref. [18].

The two-site DMFT is not restricted to the critical point  $U = U_c$  but it is able to get a consistent description of the metallic Fermi liquid for weak coupling. For the paramagnetic case at half-filling, the self-energy of the two-site model (8) can be calculated analytically

$$\Sigma_\sigma(\omega) = \frac{U}{2} + \frac{U^2}{4} \frac{\omega}{\omega^2 - (V_\sigma + 2V_\sigma)^2}. \quad (19)$$

Then the quasi-particle weight is given by

$$Z_\sigma = \left( 1 - \frac{d\Sigma_\sigma(0)}{d\omega} \right)^{-1} = \frac{1}{1 + \frac{U^2}{4(V_\sigma + 2V_\delta)^2}}. \quad (20)$$

Together with Eq. (9) this forms a set of equations to determine  $V_\sigma$  and  $Z_\sigma$ . In particular, for the symmetric case  $r=1$  this leads to

$$Z_\uparrow = Z_\downarrow = 1 - \frac{U^2}{U_c^2}, \quad (21)$$

which is qualitatively agreement with the full DMFT and improves on the result of the Gutzwiller method [19].

Knowledge of the impurity Green function (10) also allows us to calculate the double occupancy

$$d = \frac{2(V_\uparrow + V_\downarrow)^2}{U^2}. \quad (22)$$

Note that the results (19)–(22) are obtained up to second order in  $V_\sigma/U$ ,  $\sigma = \uparrow, \downarrow$ .

### 3. Comparison with the full DMFT

Here we estimate the reliability of the two-site DMFT by comparing the results of the critical interaction, the quasi-particle weight and the double occupancy with the ones obtained from the full DMFT [11].

By putting  $t_\downarrow = 0$ , expression (18) gives the exact result  $U_c = 2t_\uparrow = D$  (with  $D$  the half-width of the semicircular density of states) for the Falikov–Kimball model on the Bethe lattice. For  $r=0$ , the AHM reduces to the FKM, and the two-site DMFT calculation gives exact value of critical interaction,  $U_c = D$ . For  $0 < r \leq 1$ , the analytical results for  $U_c$  of the two-site DMFT (18) are compared with the result of numerical solutions of the full DMFT [11] in Fig. 1. As was noted in Ref. [11], the AHM at low  $T$  qualitatively behaves as the HM and has two critical Mott transition boundaries  $U_{c1}$  and  $U_{c2}$  that define a region of coexistence of metallic and insulating solutions. In addition, the Mott MIT occurs at  $U = U_{c2}$  as a continuous transition at  $T=0$ . In this paper, we consider only the Mott MIT at zero temperature, therefore we will compare our results with the critical value  $U_{c2}$  from Ref. [11]. The result from the two-site DMFT is in very good agreement with the full DMFT results over the whole  $r$  range. In addition, for  $r=1$ , from Eq. (18), the Mott transition occurs at  $U_c = 3D$  and this result is also very close

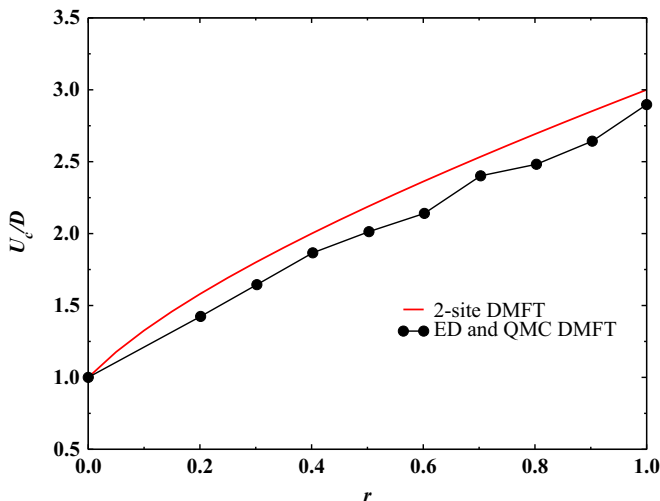


Fig. 1. Critical interaction  $U_c/D$  in the half-filled AHM at zero temperature as a function of the hopping asymmetry  $r$ : a comparison between the two-site and the full DMFT results in Ref. [11].

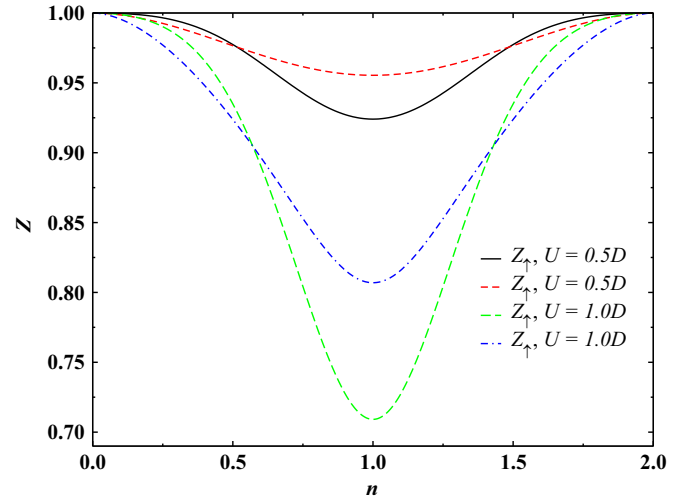


Fig. 2. Quasi-particle weight  $Z_\sigma$  at the Fermi level as a function of the total band filling  $n = n_\uparrow + n_\downarrow$  for  $r=0.4$  with some different values of the interaction strength  $U/D$ .

to the result of the projective self-consistent method [20],  $U_c = 2.92D$ , and to the result of the numerical renormalization group calculation [21],  $U_c = 2.94D$ .

We plot in Fig. 2 the quasi-particle weight  $Z_\sigma$  at the Fermi level as a function of the total band filling  $n = n_\uparrow + n_\downarrow$  for  $r=0.4$  with some different values of the interaction strength  $U/D$ . For total band filling  $n=0$  (or 2),  $Z_\uparrow = Z_\downarrow = 1$  because the interaction  $U$  has no effect on empty (full) band. Whereas for  $0 < n < 2$ , the light (spin up) and the heavy (spin down) particles are renormalized by the interaction  $U$ , especially when the system is half-filled, i.e.  $n=1$ . The renormalization of the light and the heavy particles depends on the total band filling  $n$ . If  $n$  is close to 0 (or 2), we obtained that  $Z_\downarrow < Z_\uparrow$ . It is expected as heavy fermions are more sensitive to the correlations. When the system is half-filled, however, it is essentially opposite, i.e.  $Z_\downarrow > Z_\uparrow$ . The latter can be understood because when the system is half-filled (or close) and the correlation is strong enough, we are forced to move the heavy fermions as soon as we move the light ones. It is due to the fact that at half-filling and the correlation is strong the double occupancy is small, as noted in [10]. For more detailed explanation on the anomalous effect of the quasiparticle weights, i.e.  $Z_\downarrow > Z_\uparrow$ , we refer the reader to Ref. [10]. We now discuss only the half-filled case. The obtained results for the quasi-particle weight of both spin species with  $r=0.4$  are shown in Fig. 3. Although the two-site DMFT overestimates the quasi-particle weight in the whole  $U$  range, as in [10,11] we find that electrons with smaller hopping have a larger quasi-particle weight (i.e., they are less renormalized). In addition, the quasi-particle weights vanish simultaneously at the critical point  $U_c$ . Next, we also compute the double occupancy  $\langle n_\uparrow n_\downarrow \rangle$  which is a characteristic quantity of the Mott insulating state, and compare with those obtained by the full DMFT. The numerical results for  $r=0.4$  and  $r=1$  are plotted in Fig. 4. In non-interacting case ( $U = 0$ ), the double occupancy is quarter since the empty, single occupied and double occupied states are equally realized. Introducing the interaction, the quantity of both methods rapidly decreases until  $U < U_c$ , indicating a metallic region. For  $U > U_c$ , while the double occupancy of the full DMFT remains low and weakly  $U$ -dependent, this quantity of the two-site DMFT equals zero. We will take this up in the next section.

### 4. Critical behavior near the Mott transition

We discuss the critical behavior of the quasi-particle weight

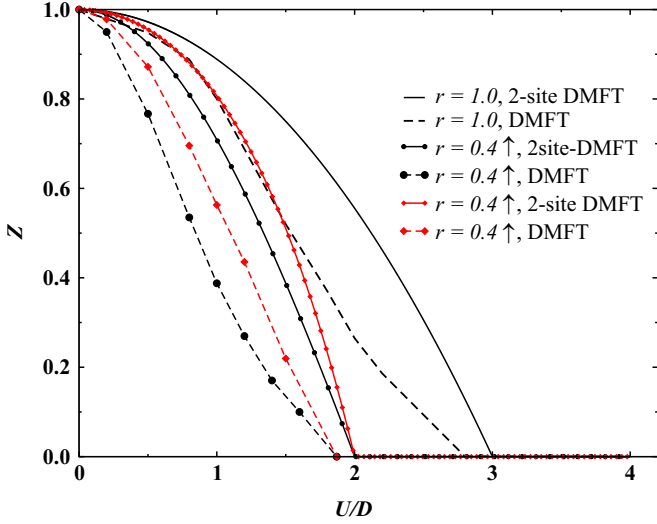


**Fig. 3.** Quasi-particle weight  $Z_\sigma$  at the Fermi level as a function of the interaction strength  $U/D$  for  $r=0.4$ : a comparison between the two-site and the full DMFT results in Ref. [11].

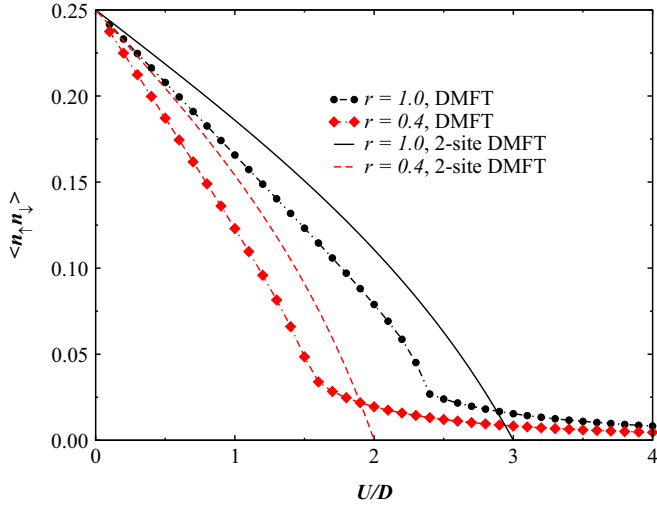


**Fig. 4.** Double occupancy as a function of the interaction strength  $U/D$  for  $r=0.4$ , 1: a comparison between the two-site and the full DMFT results in Ref. [11].

and the double occupancy in the vicinity of the Mott transition at half-filling in the AHM. To this end, we need the result of the quasi-particle weight up to fourth order in  $V$  (see Appendix A):

$$Z_\sigma = \frac{4(V_\sigma + 2V_{\bar{\sigma}})^2}{U^2} - \frac{16(V_\sigma + 2V_{\bar{\sigma}})^4 + 32V_\sigma^2(V_\sigma + 2V_{\bar{\sigma}})^2}{U^4}. \quad (23)$$

Substituting  $\sigma = \uparrow, \bar{\sigma} = \downarrow, V_i = \lambda V_i$  in (23), after some algebra we obtain

$$Z_\uparrow(r, U) = \gamma_1(r)(1 - U/U_c), \quad (24)$$

near  $U_c$  for  $U < U_c$ . Here the coefficient  $\gamma_1(r)$  is obtained analytically as a function of  $r$

$$\gamma_1(r) = \frac{2(2\lambda + 1)^2}{(2\lambda + 1)^2 + 2}, \quad (25)$$

where in the vicinity of  $U_c$

$$\lambda = \frac{1}{4}(r - 1 + \sqrt{1 + 14r + r^2}). \quad (26)$$

Similarly, near  $U_c$  for  $U < U_c$  one has

$$Z_\downarrow(r, U) = \gamma_1(r)(1 - U/U_c), \quad (27)$$

where

$$\gamma_1(r) = \frac{\lambda^2 \gamma_1(r)}{r^2}. \quad (28)$$

Combining (9), (22), (24) and (27) this also yields the result for the double occupancy near  $U_c$  for  $U < U_c$

$$d(r, U) = \gamma_d(r)(1 - U/U_c), \quad (29)$$

with the coefficient

$$\gamma_d(r) = \frac{\gamma_1(r)(\lambda + 1)^2}{2(2\lambda + 1)^2}. \quad (30)$$

For the symmetric case  $r=1$  we obtain  $\gamma_1 = \gamma_1 = \frac{18}{11}$  are the same values as those for the Hubbard model obtained in Ref. [15]. This analytic result is smaller than  $\gamma = 2$  obtained from the Brinkman–Rice approach [19], but larger than  $\gamma = 0.9 \pm 0.15$  from projective self-consistent method [20]. To our knowledge, a precise value of  $\gamma$  is not obtained for the present. For  $0 < r < 1$  since  $\frac{\lambda}{r} > 1$ , from (28) it follows that  $\gamma_1(r) < \gamma_1(r)$  which consistent with  $Z_\uparrow < Z_\downarrow$  as previously indicated. In addition, from (25) and (26) it can be verified that  $\frac{d\gamma_1}{dr} = \frac{d\gamma_1(\lambda)}{d\lambda} \frac{d\lambda}{dr}$  is positive, consequently  $\gamma_1(r)$  is a monotonically increasing function of  $r$ . Indeed, for a fixed  $t_\perp$  with increasing  $r$ ,  $U_c/t_\perp$  increases, then,  $\gamma_1(r)$  increases due to the increasing correlation effect. Similarly, for a fixed  $t_\perp$  with increasing  $r$ ,  $U_c/t_\perp$  decreases, then,  $\gamma_1(r)$  decreases due to the decreasing correlation effect. As a result, we obtain  $\frac{2}{3} < \gamma_1(r) < \frac{18}{11} < \gamma_1(r) < \frac{8}{3}$  for  $0 < r < 1$ . It has been established that in the Hubbard model the quasi-particle weight  $Z$  vanishes linearly at  $U_c$  [22]. Here for the first time we find that near Mott transition the quasi-particle weights  $Z_\uparrow$  and  $Z_\downarrow$  in the AHM with  $r \neq 0$  qualitatively behaves as  $Z$  in the HM. Furthermore, the coefficient  $\gamma_1(r)(\gamma_1(r))$  is a monotonically increasing (decreasing) function of  $r$ .

Concerning the behavior of the double occupancy near  $U_c$ , the two-site DMFT result  $\gamma_d(1) = 4/11$  in quantitative agreement with the Brinkman–Rice result  $\gamma_d = 0.25$  in the HM. Furthermore, our  $\gamma_d(r)$  is weakly  $r$ -dependent. However, as noted in [22], due to local charge fluctuations  $d(U)$  is very small but nonzero even in the insulating phase. In the HM, the numerical results close to  $U_c$  can be written as [22]

$$d(U) \approx 0.015 + 0.235(1 - U/U_c). \quad (31)$$

This indicates that the two-site DMFT misses these local fluctuations, but it correctly captures a singular contribution to the double occupancy that vanishes linearly at  $U_c$ . Hence, there is reason to believe that within the two-site DMFT the trends in the metallic phase correct on the mean-field level.

## 5. Conclusions

In summary, we have applied the two-site DMFT to study the Mott–Hubbard metal–insulator transition in the half-filled AHM at zero temperature. Explicit expressions of the critical interaction  $U_c$  for the Mott transition and the local self-energy are analytically derived. It has been demonstrated that the critical interaction of the MIT in the whole range of the hopping asymmetry  $r$  obtained from this approach is in very good agreement with most accurate numerical estimates. We also numerically computed the quasi-particle weight at the Fermi level, the double occupancy as functions of the on-site interaction  $U$  for various values of  $r$  and characterize their behavior. Comparing between the two-site and the full DMFT concerning the above quantities, we have shown that, in contrast to the CPA, the two-site DMFT gives satisfactory

results for the Mott transition and the Fermi liquid phase in the considered model with a minimum computational effort. The critical behavior of the quasi-particle weights and the double occupancy in the vicinity of the MIT was calculated analytically as functions of  $U$  and  $r$ . For the symmetric case  $r=1$  we obtain that the coefficients  $\gamma_1 = \gamma_i = \frac{18}{11}$ ,  $\gamma_d = 4/11$  are the same values as those for the Hubbard model obtained in Ref. [15]. In the general case,  $\gamma_1(r)$  ( $\gamma_i(r)$ ) is found to be a monotonically increasing (decreasing) function of  $r$ .

The calculation presented here can also be applied to the AHM on other lattices or/and to the AHM with charge and spin orders. It is also interesting to apply the two-site DMFT to study the critical behavior of a doped Mott insulator near the MIT of the AHM. This is left to a future work.

## Acknowledgments

This research is funded by Vietnam National Foundation of Science and Technology Development (NAFOSTED) under Grant no. 103.01-2014.23.

## Appendix A

Here we solve the two-site Anderson model (8) in the limit  $V_\sigma \rightarrow 0$ . At half-filling, we choose  $\epsilon_{c\sigma} = 0$  and  $\epsilon_{d\sigma} = -U/2 \equiv -\Delta$  to ensure the number of  $d$  electrons  $n=1$ . We follow the procedure described in Ref. [15] to make the calculation to fourth order in  $V_\sigma$ .

The one-electron eigenstates

$$|E_{\sigma+}\rangle = \frac{V_\sigma^2}{\Delta} - \frac{V_\sigma^4}{\Delta^3}, \quad (32)$$

$$|E_{\sigma-}\rangle = -\Delta - \frac{V_\sigma^2}{\Delta} + \frac{V_\sigma^4}{\Delta^3}, \quad (33)$$

to fourth order in  $V_\sigma$ , with the corresponding eigenstates

$$|E_{\sigma+}\rangle = \alpha_\sigma \left\{ \frac{V_\sigma}{\Delta} \left( 1 - \frac{V_\sigma^2}{\Delta^2} \right) d_\sigma^+ + c_\sigma^+ \right\} |0\rangle, \quad (34)$$

$$|E_{\sigma-}\rangle = \alpha_\sigma \left\{ d_\sigma^+ - \frac{V_\sigma}{\Delta} \left( 1 - \frac{V_\sigma^2}{\Delta^2} \right) c_\sigma^+ \right\} |0\rangle, \quad (35)$$

where

$$\alpha_\sigma^2 = 1 - \frac{V_\sigma^2}{\Delta^2} + 3 \frac{V_\sigma^4}{\Delta^4}. \quad (36)$$

Similarly, the three-electron (one-hole) eigenenergies and the corresponding eigenstates are

$$\bar{E}_{\sigma+} = \frac{V_\sigma^2}{\Delta} - \frac{V_\sigma^4}{\Delta^3}, \quad (37)$$

$$\bar{E}_{\sigma-} = -\Delta - \frac{V_\sigma^2}{\Delta} + \frac{V_\sigma^4}{\Delta^3}, \quad (38)$$

$$|\bar{E}_{\sigma+}\rangle = \bar{\alpha}_\sigma \left\{ -\frac{V_\sigma}{\Delta} \left( 1 - \frac{V_\sigma^2}{\Delta^2} \right) d_\sigma + c_\sigma \right\} |4\rangle, \quad (39)$$

$$|\bar{E}_{\sigma-}\rangle = \bar{\alpha}_\sigma \left\{ d_\sigma + \frac{V_\sigma}{\Delta} \left( 1 - \frac{V_\sigma^2}{\Delta^2} \right) c_\sigma \right\} |4\rangle, \quad (40)$$

where

$$\bar{\alpha}_\sigma^2 = 1 - \frac{V_\sigma^2}{\Delta^2} + 3 \frac{V_\sigma^4}{\Delta^4}, \quad (41)$$

and  $|4\rangle = d_\uparrow^+ d_\uparrow^+ c_\uparrow^+ c_\uparrow^+ |0\rangle$ .

For the two electron states, we use the following basic set:

$$|\phi_1\rangle = \frac{1}{\sqrt{2}} (d_\uparrow^+ c_\uparrow^+ - d_\downarrow^+ c_\uparrow^+) |0\rangle, \quad (42)$$

$$|\phi_2\rangle = \frac{1}{\sqrt{2}} (d_\uparrow^+ c_\uparrow^+ + d_\downarrow^+ c_\uparrow^+) |0\rangle, \quad (43)$$

$$|\phi_3\rangle = c_\uparrow^+ c_\uparrow^+ |0\rangle, \quad (44)$$

$$|\phi_4\rangle = d_\uparrow^+ d_\uparrow^+ |0\rangle. \quad (45)$$

The eigenenergies are given by the solutions of the equation

$$\begin{vmatrix} -\Delta - E & 0 & V^+ & V^+ \\ 0 & -\Delta - E & V^- & -V^- \\ V^+ & V^- & -E & 0 \\ V^+ & -V^- & 0 & -E \end{vmatrix} = 0, \quad (46)$$

where  $V^\pm = (V_\uparrow \pm V_\downarrow)/\sqrt{2}$ . The ground state eigenenergy and the corresponding singlet ground state is

$$E_0 = -\Delta - \frac{(V_\uparrow + V_\downarrow)^2}{\Delta} + \frac{(V_\uparrow + V_\downarrow)^4}{\Delta^3}, \quad (47)$$

$$|E_0\rangle = \sum_{j=1}^4 a_{0j} |\phi_j\rangle = \alpha_0 \left\{ |\phi_1\rangle - \frac{V_\uparrow + V_\downarrow}{\sqrt{2}\Delta} \left( 1 - \frac{(V_\uparrow + V_\downarrow)^2}{\Delta^2} \right) |\phi_3\rangle - \frac{V_\uparrow + V_\downarrow}{\sqrt{2}\Delta} \left( 1 - \frac{(V_\uparrow + V_\downarrow)^2}{\Delta^2} \right) |\phi_4\rangle \right\}, \quad (48)$$

with

$$\alpha_0^2 = 1 - \frac{(V_\uparrow + V_\downarrow)^2}{\Delta^2} + 3 \frac{(V_\uparrow + V_\downarrow)^4}{\Delta^4}. \quad (49)$$

When a  $d_\uparrow$  electron is removed from the ground state  $|E_0\rangle$ , there are two possible final states:  $|E_{1+}\rangle$  and  $|E_{1-}\rangle$ . Correspondingly, there are two possible single-hole excitations with energies,

$$E_{1+} - E_0 = \Delta + \frac{V_\uparrow^2 + (V_\uparrow + V_\downarrow)^2}{\Delta} - \frac{V_\uparrow^4 + (V_\uparrow + V_\downarrow)^4}{\Delta^3} \equiv -\epsilon_{1\uparrow}, \quad (50)$$

$$E_{1-} - E_0 = \frac{(V_\uparrow + V_\downarrow)^2 - V_\downarrow^2}{\Delta} + \frac{V_\downarrow^4 - (V_\uparrow + V_\downarrow)^4}{\Delta^3} \equiv -\epsilon_{2\uparrow}. \quad (51)$$

The transition probabilities are calculated as

$$|\langle E_{1+} | d_\uparrow | E_0 \rangle|^2 = \frac{1}{2} - \frac{(2V_\uparrow + V_\downarrow)^2}{2\Delta^2} + \frac{(2V_\uparrow + V_\downarrow)^4 + 2V_\downarrow^2(2V_\uparrow + V_\downarrow)^2}{2\Delta^4} \equiv z_{1\uparrow}, \quad (52)$$

$$|\langle E_{1-} | d_\uparrow | E_0 \rangle|^2 = \frac{(2V_\downarrow + V_\uparrow)^2}{2\Delta^2} - \frac{(2V_\downarrow + V_\uparrow)^4 + 2V_\uparrow^2(2V_\downarrow + V_\uparrow)^2}{2\Delta^4} \equiv z_{2\uparrow}, \quad (53)$$

to fourth order in  $V_\sigma$ .

When a  $d, \uparrow$  electron is added to the ground state  $|E_0\rangle$ , possible final states are  $|\bar{E}_-\rangle$  and  $|\bar{E}_+\rangle$ . Correspondingly, there are two possible single-particle excitations with energies,

$$\bar{E}_{i-} - E_0 = \frac{(V_\uparrow + V_\downarrow)^2 - V_\uparrow^2}{\Delta} + \frac{V_\downarrow^4 - (V_\uparrow + V_\downarrow)^4}{\Delta^3} \equiv \varepsilon_{3\uparrow} = -\varepsilon_{2\uparrow}, \quad (54)$$

$$\bar{E}_{i+} - E_0 = \Delta + \frac{V_\uparrow^2 + (V_\uparrow + V_\downarrow)^2}{\Delta} - \frac{V_\downarrow^4 + (V_\uparrow + V_\downarrow)^4}{\Delta^3} \equiv \varepsilon_{4\uparrow} = -\varepsilon_{1\uparrow}, \quad (55)$$

to fourth order in  $V_\sigma$ . The transition probabilities are calculated as

$$|\langle \bar{E}_{i-} | d_\uparrow^\dagger | E_0 \rangle|^2 = \frac{(2V_\downarrow + V_\uparrow)^2}{2\Delta^2} - \frac{(2V_\downarrow + V_\uparrow)^4 + 2V_\uparrow^2(2V_\downarrow + V_\uparrow)^2}{2\Delta^4} \equiv z_{3\uparrow} \\ = z_{2\uparrow}, \quad (56)$$

$$|\langle \bar{E}_{i+} | d_\uparrow^\dagger | E_0 \rangle|^2 = \frac{1}{2} - \frac{(2V_\downarrow + V_\uparrow)^2}{2\Delta^2} + \frac{(2V_\downarrow + V_\uparrow)^4 + 2V_\uparrow^2(2V_\downarrow + V_\uparrow)^2}{2\Delta^4} \\ \equiv z_{4\uparrow} = z_{1\uparrow}, \quad (57)$$

to fourth order in  $V_\sigma$ . From Eqs. (50)–(57), we obtain the  $d_\uparrow$ -electron Green function which has four poles:

$$G_\uparrow(\omega) = \sum_{i=1,2} \left( \frac{z_{i\uparrow}}{\omega - \varepsilon_{i\uparrow}} + \frac{z_{i\uparrow}}{\omega + \varepsilon_{i\uparrow}} \right). \quad (58)$$

When  $V_\uparrow, V_\downarrow \rightarrow 0$ , low energy poles merge together at  $\pm\varepsilon_{2\uparrow} \approx 0$  with the total residue  $Z_\uparrow = 2z_{2\uparrow}$ :

$$Z_\uparrow = \frac{(2V_\downarrow + V_\uparrow)^2}{2\Delta^2} - \frac{(2V_\downarrow + V_\uparrow)^4 + 2V_\uparrow^2(2V_\downarrow + V_\uparrow)^2}{2\Delta^4}, \quad (59)$$

to fourth order in  $V_\sigma$ . The  $d_\uparrow$ -electron Green function,  $G_\uparrow(\omega)$ , is obtained by making replacement  $\sigma \leftrightarrow \bar{\sigma}$  in Eqs. (50)–(58).

Consequently, one has

$$Z_\downarrow = \frac{(2V_\uparrow + V_\downarrow)^2}{2\Delta^2} - \frac{(2V_\uparrow + V_\downarrow)^4 + 2V_\downarrow^2(2V_\uparrow + V_\downarrow)^2}{2\Delta^4}. \quad (60)$$

By using (48), the double occupancy,  $d = \langle E_0 | n_{d\uparrow} n_{d\downarrow} | E_0 \rangle$ , to fourth order in  $V$  is

$$d = \frac{(V_\uparrow + V_\downarrow)^2}{2\Delta^2} \left( 1 - 3 \frac{(V_\uparrow + V_\downarrow)^2}{\Delta^2} \right). \quad (61)$$

The number of  $d$  electron,  $n = \sum_{i=1,2;\sigma} z_{i\sigma} = 1$  as expected for the half-filled case.

## References

- [1] J. Hubbard, Proc. R. Soc. Lond. A 276 (1963) 238.
- [2] L.M. Falikov, J.C. Kimball, Phys. Rev. Lett. 22 (1969) 997.
- [3] F. Gebhard, The Mott Metal–Insulator Transition: Models and Methods, Springer, Berlin, 1997.
- [4] S.J. Gu, R. Fan, H.Q. Lin, Phys. Rev. B 76 (2007) 125107.
- [5] P. Farkasovsky, Phys. Rev. B 77 (2008) 085110.
- [6] R. Jordens, N. Strohmaier, K. Gunter, H. Moritz, T. Esslinger, Nature 455 (2008) 204.
- [7] M. Jarrel, Phys. Rev. Lett. 69 (1992) 168.
- [8] M. Caffarel, W. Krauth, Phys. Rev. Lett. 72 (1994) 1545.
- [9] R. Bulla, A.C. Hewson, Th. Pruschke, J. Phys.: Condens. Matter 10 (1998) 8365.
- [10] T.L. Dao, M. Ferrero, P.S. Cornaglia, M. Capone, Phys. Rev. A 85 (2012) 013606.
- [11] E.A. Winograd, R. Chitra, M.J. Rozenberg, Phys. Rev. B 84 (2011) 233102.
- [12] E.A. Winograd, R. Chitra, M.J. Rozenberg, Phys. Rev. B 86 (2012) 195118.
- [13] M. Potthoff, Phys. Rev. B 64 (2001) 165114.
- [14] R. Bulla, M. Potthoff, Eur. Phys. J. B 13 (2000) 257.
- [15] Y. Ono, R. Bulla, A.C. Hewson, M. Potthoff, Eur. Phys. J. B 22 (2001) 283.
- [16] Y. Ohashi, Y. Ono, Phys. Soc. J. 70 (2001) 339.
- [17] B. Velicky, S. Kirkpatrick, H. Ehrenreich, Phys. Rev. 175 (1968) 747.
- [18] I.V. Stasyuk, O.B. Hera, Eur. Phys. J. B 48 (2005) 339.
- [19] W.F. Brinkman, T.M. Rice, Phys. Rev. 2 (1970) 4302.
- [20] G. Moeller, Q. Si, G. Kotliar, M. Rozenberg, D.S. Fisher, Phys. Rev. Lett. 74 (1995) 2082.
- [21] R. Bulla, Phys. Rev. Lett. 83 (1999) 136.
- [22] A. Georges, G. Kotliar, W. Krauth, M.J. Rozenberg, Rev. Mod. Phys. 68 (1996) 13.